PAPER

Check for updates

Passive viscoelastic response of striated muscles†

Fabio Staniscia [iD] ‡*[a] and Lev Truskinovsky[b]

Muscle cells with sarcomeric structure exhibit highly non trivial passive mechanical response. The difficulty of its continuum modeling is due to the presence of long-range interactions transmitted by extended protein skeleton. To build a rheological model for muscle 'material', we use a stochastic micromodel, and derive a linear response theory for a half-sarcomere, which can be extended to the whole fibre. Instead of the first order rheological equation, anticipated by Hill on the phenomenological grounds, we obtain a novel second order equation which shows that tension depends not only on its current length and the velocity of stretching, but also on its acceleration. Expressing the model in terms of elementary rheological elements, we show that one contribution to the visco-elastic properties of the fibre originates in cross-bridges, while the other can be linked to inert elements which move in the sarcoplasm. We apply this model to explain the striking qualitative difference between the relaxation in experiments involving perturbation of length *vs.* those involving perturbation of force, and we use the values of the microscopic parameters for frog muscles to show that the model is in excellent quantitative agreement with physiological experiments.

1 Introduction

One of the simplest biological systems, that still defies the attempts to reproduce it artificially as a macroscopic material, is the striated muscle.[1] Its mechanical complexity is due to the presence of a large number of hierarchically organized microscopic sub-systems that are strongly coupled through long-range interactions.[2] This makes the task of reconstructing the macroscopic constitutive relations describing even its passive mechanical response rather challenging.[3]

A broadly used phenomenological theory of the passive viscoelastic response of striated muscles, proposed by Hill,[4–7] does not rely on coarse graining techniques,[8,9] and therefore does not offer a link between macro and micro parameters. Since Hill's rheological relation involves a single characteristic time-scale, it also does not capture the puzzling differences in the passive response exhibited by striated muscles abruptly loaded in soft (isotonic) and hard (isometric) loading devices.[10,11] Here we refer to the two complementary experimental setups: in the former one controls the force applied to the extremities of a muscle fibre while measuring the length, and in the latter the force is measured as one controls the length.

A microscopically guided stochastic approach to (passive) muscle viscoelasticity was proposed by Huxley and Simmons,[10,12,32] who assumed that the individual force producing units (myosin cross-bridges) are stochastically independent. A mean field interaction between the cross-bridges was incorporated in a closely related model by Shimizu.[13–16] The two approaches have been recently unified.[2,17–19] In the present article we use this framework to rigorously derive from a micro-model a (passive) linear rheological response theory for a muscle half-sarcomere. Our analysis builds on the work of Shiino[20] who obtained a similar linear response theory for the related model of Desai and Zwanzig;[15,16,21] other related out-of-equilibrium systems were studied in ref. 22 and 23.

Our main result is a four-element linear spring-dashpot scheme, which reproduces the mechanical behaviour of a muscle fibre subjected to a time dependent perturbation. Each element can be characterized in terms of the microscopic properties of the muscle. In contrast to the three elements classical model of Hill,[4,5] the proposed rheological equation contains not only the first but also the second order time derivatives of the macroscopic displacement.

The model is characterized by two timescales that can be associated with the characteristic times of the first two transient stages of (short time) muscle response known as phases 1 and 2 of the fast force recovery, see Fig. 1 and ref. 10 and 25–27. The presence of these two timescales reflects involvement of the two parallel passive processes: the (microscopic) conformational change in the myosin heads and the relaxation of the myofilaments in a viscous environment. The obtained

[a] LMS, École polytechnique, 91128 Palaiseau Cedex, France.
  E-mail: fabiostaniscia@gmail.com
[b] PMMH, CNRS – UMR 7636 PSL-ESPCI, 10 Rue Vauquelin, 75005 Paris, France
† Electronic supplementary information (ESI) available. See DOI: 10.1039/d1sm01527c
‡ Present address: Department of Theoretical Physics, Jožef Stefan Institute, SI-1000 Ljubljana, Slovenia.
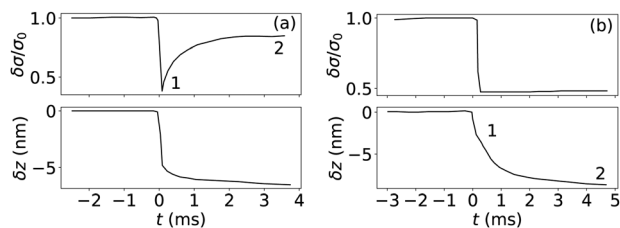
Fig. 1 Schematic representation of the first two stages (phase 1 and 2) of the transient response of a skeletal muscle subjected to an abrupt (a) isometric and (b) isotonic perturbation. Here σ is the stress and z is the elongation. (a) Adapted from ref. 24, with $\sigma_0 = 293$ kN m^{-2}, (b) adapted from ref. 11, with $\sigma_0 = 230$ kN m^{-2}.

rheological equation provides an explanation for the longterm puzzle that the fast phase of the relaxation in isotonic conditions is slower than in isometric conditions, and for the fact that phase 1 is truly instantaneous only in the isometric case. Furthermore we use the values of the microscopic parameters for frog muscles to show that our macroscopic model, which does not depend on any parameter fitting, is in quantitative agreement with physiological experiments. In addition to delivering the macroscopically adequate description, the proposed minimal model also reveals the microscopic origin of the viscoelastic response and explains its perplexing anomalies.

2 The microscopic model

The striated muscle is a hierarchical chemo-mechanical system with the smallest scale represented by force generating half-sarcomeres.[2,28] The latter can be viewed as a scaffold of parallel thin actin filaments intermingled with another scaffold of parallel thick myosin filaments. This configuration allows protruding myosin heads to attach to the binding sites on actin filaments, forming cross-bridges which can cause muscle contraction either passively, by a conformational change (power stroke), or actively, by detaching and reattaching to a new binding site.[2,29] While the cross-bridges are essentially active elements, we can still interpret their mechanical response as passive at the timescales of fast force recovery (~ 1 ms)[30]. The cross-bridges' active behaviour, involving detachment of the cross-bridges, becomes dominant only at timescales of the order of 40 ms.[31]

To reproduce the passive response of this molecular machine we use a simple microscopic model[17–19,32,33] based on Huxley–Simmons' theory.[10] It relies on an assumption that the fast force recovery (transition from phase 1 to phase 2 in Fig. 1), which is due exclusively to the power stroke, can be modeled as a mechanical response of a passive bistable system.

Following this approach we represent the pre- and post-power stroke states of each muscle cross-bridge as two isolated minima of a potential $V(x)$. The asymmetry of such potential (bias, maintained actively) allows the system to generate (stall) force in the physiological regime of isometric contractions. It is known that the cross-bridge configurations are more numerous,[26,29,34] but given that all these different configurations
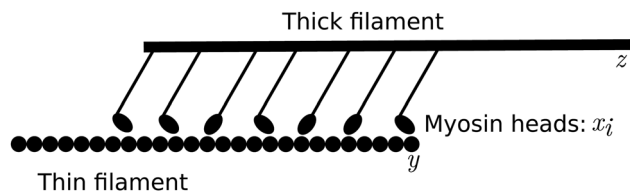
Fig. 2 Simple schematic of the model described by (1). See Section S1 of the ESI† for a detailed one.

are fundamentally similar,[11] introducing just two neighbouring states will prove to be enough to characterize the main relaxation timescales.

We model the half-sarcomere as a bundle of thick and thin filaments linked by N cross-bridges, as shown schematically in Fig. 2. In view of our focus on passive behaviour only, and following Huxley and Simmons, we include in the description only cross-bridges that are attached. The detailed description of this model is presented in Section S1 of the ESI,† while here we proceed with the study of the reduced version of the model with some of the fast degrees of freedom already relaxed.

We assume that in isometric conditions the half-sarcomere can be described by the energy:

$$E = \sum_{i=1}^{N} \left[V(x_i) + \frac{\kappa_c}{2}(y - x_i)^2 \right] + \frac{\kappa_f}{2}(z - y)^2. \quad (1)$$

Here the variables x_i represent the configuration of individual cross-bridges, and z is the position of the thick filaments backbone. The variable y characterizes the displacement of the part of the thin filaments which is bound to the cross-bridges (see Fig. 2). The first quadratic term in (1), which couples it with the x_i through a spring with a stiffness κ_c, has the effect of creating a mean field type interaction between the cross-bridges. As detailed in Section S1 of the ESI† the quantity $z - y$ mimics the elastic stretch of the filaments, which have a combined stiffness denoted by κ_f. In view of its association with macroscopic elasticity, we can consider that the variable y relaxes instantaneously,[35,36] so it can be adiabatically eliminated (Section S1 of the ESI†) and replaced by its equilibrium value:

$$y = \frac{N\kappa_c \langle x \rangle + \kappa_f z}{N\kappa_c + \kappa_f}, \quad (2)$$

where we introduced the notation:

$$\langle x \rangle = \frac{1}{N} \sum_{i=1}^{N} x_i. \quad (3)$$

If instead of isometric system we consider the system in isotonic conditions, loaded with the tension σ, we should work with the potential:

$$H = E - z\sigma A \quad (4)$$

where A is the cross sectional area of the sarcomere.

To simplify the analytical expressions we can define dimensionless units by rescaling the lengths by the size of the maximum size of the power stroke a and the energy by $\kappa_c a^2$. In these new units: $\kappa_c \to 1$ and $\kappa_f \to \lambda_f N \equiv \kappa_f/\kappa_c$.

Finally, we note that since $z(t)$ is also a macro-variable, (given that filaments are much larger than myosin heads), its dynamics can be considered deterministic and is then governed by the relaxation equation:

$$\nu\frac{\mathrm{d}z}{\mathrm{d}t} = -\frac{\partial H}{\partial z} = \lambda_f N\frac{\langle x\rangle - z}{1 + \lambda_f} + A\sigma. \tag{5}$$

Here we use the non-dimensionalized time variable normalized by the time scale γ_x/κ_c, where γ_x is the friction coefficient associated with viscous interaction of individual myosin heads with the surrounding sarcoplasm. Then $\nu \equiv \gamma_z/\gamma_x$ is the dimensionless viscosity coefficient of the whole filament. This equation is written using H as the potential, however it can be naturally adjusted to isometric conditions. We note that the timescale

$$\tau_z = \frac{\nu(1 + \lambda_f)}{\lambda_f N} \tag{6}$$

characterizes the evolution of the macro-variable z and it will be one of the two main timescales of our macroscopic rheological model.

For the evolution of the micro-variables x_i, we use the equation:

$$\dot{x}_i = -\frac{\partial H}{\partial x_i} + \xi_i = -\frac{\partial E}{\partial x_i} + \xi_i, \tag{7}$$

valid in both isometric and isotonic conditions. Here we account for the thermal noise ξ_i, characterized by the standard relations $\langle\xi_i\rangle = 0$ and $\langle\xi_i(t)\xi_j(t')\rangle = (2/\beta)\delta(t - t')\delta_{ij}$; β is the inverse dimensionless temperature. The characteristic timescale of the microscopic dynamics τ_x will be introduced later in the paper.

Our goal is to relate the small perturbations in macroscopic tension $\delta\sigma(t) = \sigma(t) - \sigma_0$ with those in macroscopic position $\delta z(t) = z(t) - z_0$, where σ_0 and z_0 are the equilibrium values. The corresponding 'rheological' relation between $\delta z(t)$ and $\delta\sigma(t)$ should involve averaging over the noise and can be expected to emerge in the form of a deterministic differential equation. The ultimate goal is to rationalize the typical physiological experiments, like those shown in Fig. 1 (see ref. 25 and 37 for other possible applications) and relate the rheological macroparameters with their microscopical analogs.

3 The rheological model

Under the assumption that N is large, the single particle probability density $p(x, t)$ can be found from the non-linear Fokker-Planck equation[20,21,38,56,57]

$$\frac{\partial p}{\partial t} = \frac{\partial}{\partial x}\left[\left(\frac{\partial V}{\partial x} + x - \frac{\langle x\rangle + \lambda_f z}{1 + \lambda_f} + \frac{1}{\beta}\frac{\partial}{\partial x}\right)p\right], \tag{8}$$

whose derivation is recalled for convenience in Section S2 of the ESI.† Here we express $\langle x\rangle = \int\mathrm{d}xpx$, which is equivalent to (3), and shows that there is a backbone induced mean-field type interaction of each cross-bridge with all other cross-bridges.

The stationary solution of (8) is:

$$p_s(x) = Z^{-1}\exp(-\beta U), \tag{9}$$

where Z is a normalization constant and $U(x, z)$ is the effective cross-bridge potential:

$$U(x, z) = V(x) + \frac{1}{2}\left(x - \frac{\langle x\rangle_s(z) + \lambda_f z}{1 + \lambda_f}\right)^2. \tag{10}$$

Here $\langle x\rangle_s$ is the equilibrium value of $\langle x\rangle$, which satisfies the self-consistence condition $\langle x\rangle_s = \int\mathrm{d}xp_s(x)x$.[39]

After the equilibrium properties are established, we can develop the linear response theory using as a starting point the approach developed in ref. 20. To linearise (8) we consider a small perturbation $\delta p(x, t) = p(x, t) - p_s(x)$, associated with a small change of the macroscopic displacement variable $\delta z(t)$. The linear equation describing such perturbation is:

$$\frac{\partial\delta p}{\partial t} = L\delta p - \frac{1}{1 + \lambda_f}\frac{\partial p_s}{\partial x}\left(\int\mathrm{d}xx\delta p + \lambda_f\delta z\right), \tag{11}$$

where we defined the operator L:

$$Lp = \frac{\partial}{\partial x}\left[\left(\frac{\partial V}{\partial x} + x - \frac{\langle x\rangle_s + z\lambda_f}{1 + \lambda_f} + \frac{1}{\beta}\frac{\partial}{\partial x}\right)p\right]. \tag{12}$$

Using (11) one can show that the evolution of the average configuration of a cross-bridge $\langle\delta x\rangle(t) = \int\mathrm{d}xx\delta p(x, t)$ is described by:

$$\langle\delta x\rangle(t) = \int_{-\infty}^{\infty}\frac{\langle\delta x(t')\rangle + \lambda_f\delta z(t')}{1 + \lambda_f}\chi_{xx}(t - t')\mathrm{d}t', \tag{13}$$

where

$$\chi_{xx}(t) = -\Theta(t)\int\mathrm{d}xx\mathrm{e}^{Lt}\frac{\partial}{\partial x}p_s(x), \tag{14}$$

is the susceptibility and $\Theta(t)$ is the Heaviside function. In Fourier space (13) reads

$$\langle\delta x\rangle(\omega) = \frac{\lambda_f\chi_{xx}(\omega)\delta z(\omega)}{1 + \lambda_f - \chi_{xx}(\omega)}. \tag{15}$$

Next we write the conventional fluctuation–dissipation type identity (see Section S3 of the ESI† and ref. 20)

$$\chi_{xx} = -\beta\Theta(t)\frac{\mathrm{d}S_{xx}}{\mathrm{d}t}, \tag{16}$$

where

$$S_{xx}(t) = \langle x(t)x(0)\rangle - \langle x\rangle_s^2 \tag{17}$$

is the auto-correlation function of a single cross-bridge. Given that in linear approximation each cross-bridge can be viewed as conducting independently a Brownian motion in a double well potential, we can use the Kramers approximation to obtain:[40,41]

$$S_{xx}(t) \simeq l_U^2\mathrm{e}^{-\frac{t}{\tau_x}} + d^2\mathrm{e}^{-\frac{t}{\tau_0}} \tag{18}$$

(see Section S4 of the ESI† and ref. 42), where

$$\tau_x \simeq \frac{2\pi}{\sqrt{|U''(x_M)|}}\frac{\mathrm{e}^{\beta U(x_M)}}{\sqrt{U''(x_0)}\mathrm{e}^{\beta U(x_0)} + \sqrt{U''(x_1)}\mathrm{e}^{\beta U(x_1)}}, \tag{19}$$

characterizes kinetics of the the barrier crossing while $\tau_0 \simeq 1/U''(x_{0,1})$ characterizes the kinetics of relaxation inside a single

well (with $x_{0,1}$ being the minima of the potential (10) and x_M the local maximum between them).

The pre-factors can be also computed explicitly (see Section S4 of the ESI†). We obtain:

$$l_U = \frac{|x_0 - x_1|\sqrt{q}}{(1+q)} \qquad (20)$$

and

$$d \simeq \sqrt{\left(\frac{1}{\beta U''(x_0)} + \frac{q}{\beta U''(x_1)}\right) \Big/ (1+q)}, \qquad (21)$$

with

$$q = \sqrt{\frac{U''(x_0)}{U''(x_1)}} e^{\beta[U(x_0)-U(x_1)]}. \qquad (22)$$

We will neglect the second term in the right hand side of (18) since in physiological conditions the relaxation within a single well is much faster ($\tau_0 \ll \tau_x$) and its effect is much smaller ($d \ll l_U$) than the corresponding effects due to the barrier crossing.

We can now rewrite (16) in the Fourier space

$$\chi_{xx}(\omega) = \frac{l_U^2 \beta}{1 + i\omega\tau_x}, \qquad (23)$$

and use (5) to obtain the desired linear response relation between the macro-variables δz and $\delta\sigma$:

$$\left[-\omega^2\tau_x\tau_z + i\omega\left(\tau_z + \tau_x - \frac{\beta l_U^2\tau_z}{1+\lambda_f}\right) + 1 - \beta l_U^2\right]\delta z(\omega)$$
$$= \left[i\omega\tau_x\frac{1+\lambda_f}{\lambda_f N} + \frac{1+\lambda_f - \beta l_U^2}{\lambda_f N}\right]A\delta\sigma(\omega). \qquad (24)$$

In the real space the resulting rheological relation can be rewritten in the form:

$$\theta\eta_f\frac{d^2}{dt^2}\delta z + (\theta E_f + \eta_f)\frac{d}{dt}\delta z + C\delta z = \delta\sigma + \theta\frac{d}{dt}\delta\sigma \qquad (25)$$

where

$$C = \frac{E_c E_f}{E_c + E_f}, \quad \theta = \frac{\eta_c}{E_c + E_f}. \qquad (26)$$

The expression of the rheological model (25) in this from allows one to interpret the coefficients

$$E_c = N(1 - \beta l_U^2)/(\beta l_U^2 A)$$
$$E_f = N\lambda_f/(A + A\lambda_f)$$
$$\eta_c = N\tau_x/(\beta l_U^2 A)$$
$$\eta_f = \nu/A \qquad (27)$$

as describing the components of a spring-dashpot model shown in Fig. 3. The next step is to use the available microscopic data on molecular components for the quantitative interpretation of the results of the macroscopic physiological experiments with actual muscle fibers. We notice in this respect that (25) is a relation between the displacement and the stress,
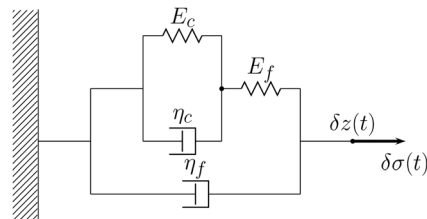
Fig. 3 Schematic representation of the rheological model (25).

and not between the strain and the stress as in usual rheological models. Therefore, to obtain the elastic moduli one has to multiply the values of E_c and E_f by the length of a half-sarcomere l_0 and similarly normalize the kinematic viscosities η_c and η_f.

4 Physical interpretation

The proposed rheological model, which provides a relation between the perturbations of tension and position, involves (see Fig. 3) at the inner level a parallel bundle of an elastic element E_c and a dashpot with viscosity η_c, and at the outer level a spring with elastic element E_f and a dashpot with viscosity η_f.

The inner level of Fig. 3 accounts for the cross-bridge dynamics, since it comes from the linearisation of (8), and its elements depend on the properties of cross-bridges. For instance E_c characterizes the elasticity of myosin heads' configuration. It depends on the parameter l_U, which is an effective width of the potential (10). This quantity is finite if the two minima have comparable energy, which means that the cross-bridge can actually switch between them. Instead, its value is close to zero if one of the two energies is much larger than the other and in this case the system will not fluctuate between the two states. Under such conditions, which are not physiological, the dynamics would be dominated by the term d, describing the amplitude of fluctuations within the single wells. Note also that η_c is an effective viscosity which sets the timescale θ of the cross-bridge dynamics. It depends exponentially on the height of energy barrier between the configurations of the cross-bridges (through τ_x), and has the effect of delaying their adaptation to external perturbations. Overall, we can conclude that for small perturbations the cross-bridge dynamics can be described by a Kelvin–Voigt model.

The outer level in Fig. 3 represents the dynamics of the filaments described by (5). Here E_f is the combined stiffness of cross-bridges and myofilaments per unit area, which ties the backbone position δz with the average cross-bridge position $\langle\delta x\rangle$, while η_f is characteristic of the friction felt by the filaments as they move in the sarcoplasm. If $\nu = \eta_f = \tau_z = 0$, (25) reproduces the rheological structure of the (passive) Hill's model.

To make a quantitative comparison between the model (25) and the Hill's model, we can define in isometric conditions the storage modulus G_H' and the loss modulus G_H'' as real and imaginary parts of the ratio $A\delta\sigma(\omega)/\delta z(\omega)$; in isotonic conditions to obtain the similar quantities G_S' and G_S'' we must consider
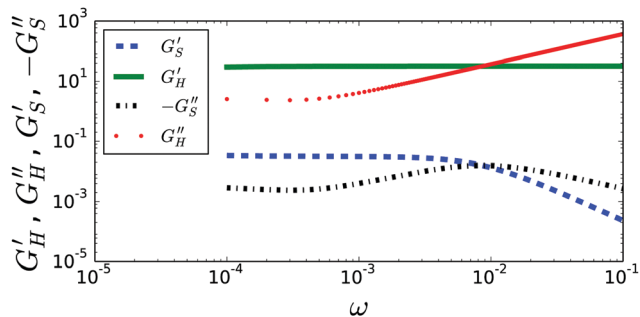
Fig. 4 Frequency dependence of the loss and storage moduli in isometric and isotonic conditions for the physiological choice of parameters.

instead the ratio $\delta z(\omega)/A\delta\sigma(\omega)$. The frequency dependence of these parameters is illustrated in Fig. 4. Note the divergence of G''_H at large ω in qualitative difference with the Hill's model where this parameter tends to zero. Similarly, in the Hill's model G'_S has a finite limit at large ω while in our model it tends to zero. We also note that the entropy production in the system scales with the loss modulus G''_H and the fact that the latter is always positive insures the thermodynamic consistency of the macroscopic rheological model.

While the rheological eqn (25) was obtained for a single half-sarcomere, it can be renormalized to the scale of a muscle fibre. To this end we need to assume that the response is affine, at least when perturbations are sufficiently small. We can then view a myofibril as a chain of $L \sim 10^4$ half-sarcomeres connected in series, and represent a muscle fibre by a parallel arrangement of $M \sim 200$–2000 such myofibrils. The renormalization will then reduce to the substitution $\delta z \rightarrow \delta z/L$ with $\delta\sigma$ remaining unchanged.

5 Tensorial form

Viewing muscle as a passive viscoelastic bulk material we can rewrite the rheological relation (25) in the tensorial form. Given that our focus is on liner response, we can neglect the non-linear effects, for instance the ones associated with objective time derivatives. Under the assumption that the deformation is incompressible we need to relate the deviatoric part of the Cauchy stress tensor σ_{ab} with the deviatoric part of the strain tensor $\varepsilon_{ab} = (1/2)(u_{ab} + u_{ba})$, where $a, b = 1, 2, 3$, $u_{ab} = \partial u_a/\partial r_b$, r_b is the position vector and u_a is the displacement vector.

We can describe the rheological response of the outer layer by the differential relation

$$\sigma_{ab} = D^e_{abcd}\dot{\varepsilon}_{cd} + E^e_{abcd}(\varepsilon_{cd} - \gamma^i_{cd}). \quad (28)$$

Here the superimposed dot denotes time derivative and we introduced the fourth order tensors of elastic E^e and viscous D^e moduli in the outer layer. We also introduced the inelastic deviatoric strain γ^i_{ab} developing in the inner layer of the mode. Next we introduce the deviatoric stress σ^i_{ab} in the inner layer of the model. Here we can use the standard Kelvin–Voigt model and write

$$\sigma^i_{ab} = D^i_{abcd}\dot{\gamma}^i_{cd} + E^i_{abcd}\gamma^i_{cd}, \quad (29)$$

where we introduced the tensors of elastic E^i and viscous D^i operating in the inner layer of the model. Finally, the outer and the inner layered are coupled through the stress balance relation

$$\sigma^i_{ab} = E^e_{abcd}(\varepsilon_{cd} - \gamma^i_{cd}). \quad (30)$$

It is straightforward to check that eqn (28)–(30) represent a direct tensorial generalization of the model (25) and reduce to it when the considered deformation is purely longitudinal.

To obtain a more transparent representation of the same tensorial model we can eliminate the internal strain γ^i_{ab}. We thus write the stress balance:

$$\sigma_{ab} = \sigma^l_{ab} + \sigma^u_{ab} \quad (31)$$

where $\sigma^l_{ab} = D^e_{abcd}\dot{\varepsilon}_{cd}$ is the deviatoric part of the stress produced in the outer layer due to viscous friction (lower branch of Fig. 3). Using the initial condition $u_{ab}(0) = 0$, the stress generated by the upper branch of Fig. 3 can be written in terms of the corresponding exponential tensorial kernels K and L:

$$\sigma^u_{ab} = \int_0^t (K_{abcd}(t - t')\varepsilon_{cd} + L_{abcd}(t - t')\dot{\varepsilon}_{cd})dt'. \quad (32)$$

6 Comparison with experimental data

We can use the relation (25) to calculate the response of a striated muscle fibre to canonical step-like perturbations[43] imitating in this way typical mechanical experiments.

In the isometric conditions we study the tension response to a perturbation of the sarcomere length. In our notations, one expresses the perturbation in the form:

$$\delta z(t) = \delta z_0 \Theta(t). \quad (33)$$

The response can be calculated using (25). We obtain the corresponding stress increment in the form:

$$\delta\sigma(t) = \delta z_0 \left[(E_f - C)e^{-\frac{t}{\theta}} + C + \eta_f \delta(t)\right]\Theta(t), \quad (34)$$

were $\delta(t)$ is the Dirac function; the corresponding singular contribution to the response usually cannot be detected in experiments given that the perturbation is not strictly instantaneous. Note the first jump in tension

$$\lim_{t\rightarrow 0^+} \delta\sigma(t) = E_f \delta z_0, \quad (35)$$

which takes place simultaneously with the applied length step (phase 1 in Fig. 1a). This is the signature of a purely elastic response[24] illustrated in Fig. 5a, where we compare the results of the direct numerical experiments conducted using the original microscopic model (see more about this below) with the predictions of our macroscopic rheological model. The elastic phase is followed by an exponential relaxation (phase 2 in Fig. 1a and 5a) with the timescale θ. The condition $\theta > 0$, or equivalently, $1 + \lambda_f - \beta l_U^2 > 0$, then serves as a condition (which is approximate since we are using

an approximate expression for the correlation function S_{xx}) for the mechanical stability of the equilibrium system in the hard device.

In isotonic conditions we study the response of the system to a small step-like perturbation of the tension which we can write in the form

$$\delta\sigma(t) = \delta\sigma_0\Theta(t). \tag{36}$$

The corresponding increment in displacement $\delta z(t)$ can be again calculated from (25). We obtain:

$$\delta z(t) = \delta\sigma_0\left[-\frac{\tau_+\tau_-}{\eta_f(\tau_+ - \tau_-)}\left(1 - \frac{\tau_+}{\theta}\right)e^{-\frac{t}{\tau_+}}\right.$$
$$\left. + \frac{\tau_+\tau_-}{\eta_f(\tau_+ - \tau_-)}\left(1 - \frac{\tau_-}{\theta}\right)e^{-\frac{t}{\tau_-}} + \frac{1}{C}\right]\Theta(t), \tag{37}$$

where we introduced two new effective timescales:

$$\tau_\pm = \frac{\eta_c + \eta_f}{2E_c} + \frac{\eta_f}{2E_f} \pm \sqrt{\left(\frac{\eta_c + \eta_f}{2E_c} - \frac{\eta_f}{2E_f}\right)^2 + \frac{\eta_f^2}{E_cE_f}}. \tag{38}$$

The approximate stability condition obtained from the sign of the timescales is now $1 - \beta l_U^2 > 0$. Note the difference between the stability thresholds in soft and hard device reflecting the expected ensemble inequivalence in this mean field system.[19,44]

Observe also that according to (37)

$$\lim_{t\to 0}\delta z(t) = 0, \tag{39}$$

which suggests that there is no 'synchronous' purely elastic response to a step-like tension perturbation. Instead the relaxation in the stages 1 and 2 is characterized by two-scale exponential decay with timescales τ_- and τ_+. Since $\tau_- \ll \tau_+$ the first relaxation process, associated with the timescale τ_-, has sometimes been interpreted as purely elastic. The two-scale nature of the relaxation in isotonic conditions predicted by our rheological model also explains the long known difficulty[10] of separating stages 1 and 2 in the corresponding transient

response, see the experimental Fig. 1b and the theoretical Fig. 5b. To address this puzzle more elaborate chemo-mechanical models were formulated to match the experimental data, see for instance,[37] however, none of the proposed models can be compared in simplicity with (25).

Note also that the immediate stress–strain (tension–length) response during sufficiently fast perturbations (~ 150 μs) which is usually expected to be linear elastic, shows instead a fundamental rate dependency in isotonic conditions. In other words, under such conditions there is an appreciable rate dependent delay operating already at the timescales of perturbations in physiological experiments. This effect is well known to experimentalists as it effectively drives the instantaneous response data away from a linear elastic one which would mean instantaneous relaxation.[26] We emphasize that similar effects have not been observed in the isometric experiments[25] which can be viewed as another justification of our rheological model.

Using the basic physiological and physical constraints on the parameters, $\beta \geq 0$, $\nu \geq 0$, $\lambda_f \geq 0$, one can show that in stable regimes necessarily $\tau_+ > \theta$, which is in agreement with the experimental observations that the relaxation in the soft the device is slower than in the hard device.[11,25] Our rheological model allows one to rationalize the observed difference of these two timescales: in a length perturbation the backbone position δz is controlled, and the relaxation timescale θ depends only on the rates of transitions of the cross-bridges, in other words, on the kinetics of the macro-variable variable $\langle\delta x\rangle$. Instead, after a tension perturbation, the relaxation timescale τ_+ is also affected by the viscous dynamics of the backbone variable δz. Therefore, if in the case of the hard-device, the time scale θ will effectively describe the relaxation of a single variable, in the soft-device the time scale τ_+ will characterize the relaxation of the two variables. Since we refer here to the relaxation between the same configurations, the kinetics in the soft device will be slower than in the hard device at least due to the larger dimensionality of the relevant configurational space in the former case.

6.1 Simulations

We are now in the position to evaluate to what extent the microscopic stochastic model and the macroscopic deterministic rheological model can reproduce the outcomes of the realistic experiments. Numerical simulations of the microscopic model were conducted with a second order stochastic Runge–Kutta algorithm. We simulated the response of the microscopic model to a step-like perturbation δz in a hard device, and $\delta\sigma$ in a soft device, computing the corresponding responses $\delta\sigma(t)$ and $\delta z(t)$.

The results are summarized in Fig. 5 where we compared them with the predictions of (25). We used the physiological values of parameters (for the the justification of our choices, see the next Section) with the exception that instead of the realistic value $N \sim 500\,000$, we used the computationally reachable value $N = 32\,768$, while appropriately rescaling the parameters ν and A to ensure that the behaviour is the same and that the timescale τ_z remains at its realistic value. Numerical experiments aimed at a single bundle of thick and

Fig. 5 Response to a step like perturbation in the rheological model (25) (analytical), compared with direct numerical simulations for $N = 32\,768$ cross-bridges averaged over 10 realizations (numerics). (a) Hard-device, (b) soft device.

thin filaments with $N = 128$ were performed using the same rescaling and it obtained results that were qualitatively the same. In both cases the agreement between the stochastic model and the rheological eqn (25) is excellent for both hard and soft devices.

6.2 Calibration of the model

To make quantitative predictions and compare our results with physiological measurements, we need to substitute in our model the physical values of parameters and reintroduce dimensional units. For the cross-bridge stiffness we take the value $\kappa_c = 3.29$ pN nm^{-1},[45] while the combined stiffness of actin and myosin filaments can be estimated at the value $\kappa_f \simeq 153$ pN nm^{-1}.[35,36] To estimate γ_x we assume that a typical myosin head has the diameter $h \simeq 6$ nm and that the sarcoplasm has the effective dynamical viscosity $\mu \simeq 2.3 \times 10^{-6}$ pN ms nm^{-2}.[46,47] Approximating the head as spherical we can use Stokes' law to obtain $\gamma_x \simeq 3\pi\mu h \simeq 1.3 \times 10^{-4}$ ms pN nm^{-1}. The friction coefficient for the bundle of thick filaments constituting the half-sarcomere can be now be estimated as $\gamma_z \simeq \xi A$, where $\xi \simeq 3 \times 10^{-4}$ pN ms nm^{-3} is a viscosity coefficient obtained in ref. 45 and 48–50 from experiments on unstimulated muscles, and $A \simeq 8$ μm^2. For a single thick filament we can instead take $\gamma_z = \xi/\rho_f \simeq 0.480$ ms pN nm^{-1} where $\rho_f = 2/(\sqrt{3}b^2)$ is the density of thick filaments in the cross section of a sarcomere, in which the thick filaments form a triangular pattern and lie at a distance $b = 43$ nm,[51] and $A = 1/\rho_f$.

To model the double well potential we use the simplest quartic polynomial:

$$V(x) = c_4 x^4/4 + c_3 x^3/3 + c_2 x^2 \qquad (40)$$

where the two minima are centred around $x = -a/4$ and $x = 0$ and the maximum power stroke length is $a = 11$ nm. More specifically, we assume that the bias is towards the post-power-stroke state $x = -a/4$ whose energy level is shifted down at 12.5 zJ below the energy level of pre-power-stroke state $x = 0$. The maximum between the energy minima represents the energetic barrier and defines the activation energy for the muscle power stroke. It was previously estimated to be either 55.3 zJ or 95.1 zJ.[52,53] We have chosen the smaller value as more relevant for the the fast time transient response. These estimates allow one to determine the parameters of the quartic potential V which in the dimensionless form are $c_2 \simeq 61$, $c_3 \simeq 757$ and $c_4 \simeq 2050$.

Using these values of parameters, and the temperature 273 K, we obtain the time scale $\theta \simeq 0.35$ ms which is compatible with the relaxation time measured in ref. 25. Next we estimate the elastic modulus involved in the instantaneous response of a half-sarcomere in the hard device. Given that $l_0 \simeq 1.05$ μm is the length of a half-sarcomere and $r \simeq 0.83$ is the fraction of the cross-section of the muscle fibre occupied by sarcomeres,[54] we obtain

$$E_Y = \lim_{t\to 0} \delta\sigma(t) A\rho_f r l_0/\delta z_0 \simeq N A \rho_f r \kappa_f l_0/(N\kappa_c + \kappa_f) \simeq 57 \times 10^6 \text{ N m}^{-2},$$

close to the value measured in ref. 25. Finally we compute the time scale $\tau_+ \simeq 0.44$ ms which is also in good agreement with experimental observations[26,37] and another time scale $\tau_- \simeq 0.004$ ms which has not measured before, but whose small value justifies the fact that phase 1 is usually considered instantaneous even in isotonic condition.

7 Conclusions

We have shown that the fast time viscoelastic mechanical response of striated muscles, involving such physiologically important phenomenon as the 'fast force recovery', can be quantitatively rationalized through a minimal stochastic model of the microscopic structure of a half-sarcomere. From such micro-scale model we derived a deterministic rheological model which describes linear response of muscle fibres under time dependent loading conditions and found explicit relations between the macroscopic and the microscopic parameters.

The fact that the derived rheological relation involves not only first but also second derivatives, showing rather unusual dependence of the generated force on the acceleration of the straining, allowed us for the first time to rationalize the qualitative differences in the mechanical response of isometrically and isotonically loaded muscles. The important advantage of the proposed model is that it is not phenomenological as it offers an explicit link between the macroscopic and the microscopic parameters. This allowed us to calibrate the model using the experimental data for the microscopic model, and obtained an excellent quantitative agreement with physiological observations without using fitting parameters.

It would be of interest to check experimentally the anticipated quantitative link between the mechanical response to fast perturbations[25,37] and the power spectrum of mechanical fluctuations.[55] On the theoretical side, the main challenge is to develop an adequate description of the active element which can be incorporated into the rheological model to capture the mechanical response of striated muscles at longer time scales.

Author contributions

Both authors conducted the research and wrote the paper. FS performed the computations.

Conflicts of interest

There are no conflicts to declare.

Acknowledgements

References

1 N. Kidambi, R. L. Harne and K.-W. Wang, *Phys. Rev. E*, 2018, **98**, 043001.

2 M. Caruel and L. Truskinovsky, *Rep. Prog. Phys.*, 2018, **81**, 036602.

3 F. Regazzoni, L. Dedè and A. Quarteroni, *Biomech. Model. Mechanobiol.*, 2018, **17**, 1663–1686.

4 A. V. Hill, *Proc. R. Soc. London, Ser. B*, 1938, **126**, 136–195.

5 A. V. Hill, *Proc. R. Soc. London, Ser. B*, 1949, **136**, 399–420.

6 S. A. Glantz, *J. Biomech.*, 1974, **7**, 137–145.

7 B. Gerazov and P. N. Garner, *Speech and Computer*, Cham, 2016, pp. 84–91.

8 G. P. DeVault and J. A. McLennan, *Phys. Rev.*, 1965, **137**, A724–A730.

9 F. Bavaud, *J. Stat. Phys.*, 1987, **46**, 753–775.

10 A. F. Huxley and R. M. Simmons, *Nature*, 1971, **233**, 533–538.

11 M. Reconditi, M. Linari, L. Lucii, A. Stewart, Y.-B. Sun, P. Boesecke, T. Narayanan, R. F. Fischetti, T. Irving, G. Piazzesi, M. Irving and V. Lombardi, *Nature*, 2004, **428**, 578 EP.

12 E. Eisenberg, T. Hill and Y. Chen, *Biophys. J.*, 1980, **29**, 195–227.

13 H. Shimizu and T. Yamada, *Prog. Theor. Phys.*, 1972, **47**, 350–351.

14 K. Kometani and H. Shimizu, *J. Stat. Phys.*, 1975, **13**, 473–490.

15 L. L. Bonilla, *J. Stat. Phys.*, 1987, **46**, 659–678.

16 T. Frank, *Phys. Lett. A*, 2004, **329**, 475–485.

17 L. Marcucci and L. Truskinovsky, *Phys. Rev. E: Stat., Nonlinear, Soft Matter Phys.*, 2010, **81**, 051915.

18 L. Marcucci and L. Truskinovsky, *Eur. Phys. J. E: Soft Matter Biol. Phys.*, 2010, **32**, 411–418.

19 M. Caruel, J.-M. Allain and L. Truskinovsky, *Phys. Rev. Lett.*, 2013, **110**, 248103.

20 M. Shiino, *Phys. Rev. A: At., Mol., Opt. Phys.*, 1987, **36**, 2393–2412.

21 R. C. Desai and R. Zwanzig, *J. Stat. Phys.*, 1978, **19**, 1–24.

22 A. Patelli, S. Gupta, C. Nardini and S. Ruffo, *Phys. Rev. E: Stat., Nonlinear, Soft Matter Phys.*, 2012, **85**, 021133.

23 A. Patelli and S. Ruffo, *Eur. Phys. J. D*, 2014, **68**, 329.

24 G. Piazzesi, M. Reconditi, M. Linari, L. Lucii, Y.-B. Sun, T. Narayanan, P. Boesecke, V. Lombardi and M. Irving, *Nature*, 2002, **415**, 659 EP.

25 G. Piazzesi, M. Reconditi, N. Koubassova, V. Decostre, M. Linari, L. Lucii and V. Lombardi, *J. Physiol.*, 2003, **549**, 93–106.

26 V. Decostre, P. Bianco, V. Lombardi and G. Piazzesi, *Proc. Natl. Acad. Sci. U. S. A.*, 2005, **102**, 13927–13932.

27 G. Piazzesi, M. Reconditi, M. Linari, L. Lucii, P. Bianco, E. Brunello, V. Decostre, A. Stewart, D. B. Gore, T. C. Irving, M. Irving and V. Lombardi, *Cell*, 2007, **131**, 784–795.

28 B. Alberts, D. Bray, K. Hopkin, A. D. Johnson, J. Lewis, M. Raff, K. Roberts and P. Walter, *Essential cell biology*, Garland Science, 2013.

29 A. F. Huxley, *J. Physiol.*, 1974, **243**, 1–43.

30 R. Sheshka, P. Recho and L. Truskinovsky, *Phys. Rev. E*, 2016, **93**, 052604.

31 J. Howard, *Mechanics of Motor Proteins and the Cytoskeleton*, Sinauer Associates, Publishers, 2001.

32 M. Caruel and L. Truskinovsky, *Phys. Rev. E*, 2016, **93**, 062407.

33 M. Caruel and L. Truskinovsky, *J. Mech. Phys. Solids*, 2017, **109**, 117–141.

34 M. Caremani, L. Melli, M. Dolfi, V. Lombardi and M. Linari, *J. Physiol.*, 2013, **591**, 5187–5205.

35 H. Huxley, A. Stewart, H. Sosa and T. Irving, *Biophys. J.*, 1994, **67**, 2411–2421.

36 K. Wakabayashi, Y. Sugimoto, H. Tanaka, Y. Ueno, Y. Takezawa and Y. Amemiya, *Biophys. J.*, 1994, **67**, 2422–2435.

37 G. Piazzesi, L. Lucii and V. Lombardi, *J. Physiol.*, 2002, **545**, 145–151.

38 T. D. Frank, *Nonlinear Fokker–Planck equations: fundamentals and applications*, Springer Science & Business Media, 2005.

39 T. Dauxois, S. Lepri and S. Ruffo, *Commun. Nonlinear Sci. Num. Simul.*, 2003, **8**, 375–387.

40 J. L. Skinner and P. G. Wolynes, *J. Chem. Phys.*, 1978, **69**, 2143–2150.

41 R. Pratolongo, A. Perico, K. F. Freed and A. Szabo, *J. Chem. Phys.*, 1995, **102**, 4683–4690.

42 C. W. Gardiner, *Handbook of stochastic methods*, Springer, Berlin Heidelberg New York, 1985.

43 F. Mainardi and G. Spada, *Eur. Phys. J.-Spec. Top.*, 2011, **193**, 133–160.

44 J. Barré, D. Mukamel and S. Ruffo, *Phys. Rev. Lett.*, 2001, **87**, 030601.

45 L. E. Ford, A. F. Huxley and R. M. Simmons, *J. Physiol.*, 1977, **269**, 441–515.

46 M. J. Kushmerick and R. J. Podolsky, *Science*, 1969, **166**, 1297–1298.

47 M. Arrio-Dupont, S. Cribier, G. Foucault, P. Devaux and A. d'Albis, *Biophys. J.*, 1996, **70**, 2327–2332.

48 M. A. Bagni, G. Cecchi, F. Colomo and P. Garzella, *J. Physiol.*, 1995, **482**, 391–400.

49 M. Bagni, G. Cecchi, F. Colomo and P. Garzella, *Biophys. J.*, 1992, **63**, 1412–1415.

50 M. A. Bagni, G. Cecchi, E. Cecchini, B. Colombini and F. Colomo, *J. Muscle Res. Cell Motil.*, 1998, **19**, 33–42.

51 I. Matsubara and G. F. Elliott, *J. Mol. Biol.*, 1972, **72**, 657–669.

52 R. Elangovan, M. Capitanio, L. Melli, F. S. Pavone, V. Lombardi and G. Piazzesi, *J. Physiol.*, 2012, **590**, 1227–1242.

53 M. Anson, *J. Mol. Biol.*, 1992, **224**, 1029–1038.

54 B. A. Mobley and B. R. Eisenberg, *J. Gen. Physiol.*, 1975, **66**, 31–45.

55 E. Malmerberg, C. A. Kerfeld and P. H. Zwart, *IUCrJ*, 2015, **2**, 309–316.

56 T. S. Lundgren and Y. B. Pointin, *J. Stat. Phys.*, 1977, **17**, 323–355.

57 P.-H. Chavanis, *Phys. A*, 2006, **361**, 55–80.